Korean J. Chem. Eng., 39(6), 1614-1623 (2022)
DOI: 10.1007/s11814-021-1025-8

pISSN: 0256-1115
eISSN: 1975-7220

Structural and thermal properties of the Fe-based alloys prepared by mechanical milling

Rakia Daly*,†, Juan Jose Sunol, and Mohamed Khitouni***

*Laboratoire de Chimie Inorganique, Ur-11-ES-73, Université de Sfax, FSS, BP 1171, Tunisie
**Dep. de Fisica, Universitat de Girona, Campus Montilivi, Girona 17071, Spain
(*Received 30 August 2021 • Revised 27 October 2021 • Accepted 23 November 2021*)

Abstract−Nanocrystalline FeCoNi and FeCoNiSi powdered alloys were prepared by mechanical milling process (MA). Using X-ray diffraction patterns, we experimentally proved that when MA reached a time of 50 h, it led to a decrease of the crystallite size down to 20 nm and 32 nm for FeCoNiSi and FeCoNi, respectively. However, the dislocation density increased, reaching the highest value for the alloy associated with silicon. Nevertheless, this high energy ball-milling process is not used only for the refining of microstructure, but also to induce either a chemical reaction between the powdered chemical elements or a phase transformation, such as the allotropic transformation of HCP-Co to FCC-Co and the formation of highly disordered Fe-based solid solutions. Thermal stability of the milled mixtures was investigated by DSC from 25 up to 700 °C at a heating rate of 10 °C/min. Various milled samples were first annealed at specific temperatures and then analyzed using X-ray diffraction, which demonstrated the stability of the evolved phases during subsequent heating and the formation of some metallic oxides, such as Fe_3O_4, Fe_2O_3 and FeO, particularly for the elevated annealing temperatures.

Keywords: Milling, Nanostructures Materials, Annealing, DSC, X-ray Diffraction

INTRODUCTION

Nanocrystalline alloys are integrated almost in all scientific fields, particularly in medical, electronic and information technology [1-3]. Mechanical alloying is an efficient method that can produce nanocrystalline alloys with a combination of properties making them potentially useful in a number of applications [4-8]. It is known that various Fe-based amorphous alloys can be obtained by several methods, namely electro-deposition, gas condensation, rapid solidification and mechanical alloying (MA). The latter has the advantage of relatively low-cost equipment, simplicity, low-temperature processing, great flexibility in the selection of the processing parameters, and ability to produce large quantities of material with the same physical properties [9]. The major benefit of this process is that it can be used to synthesize a variety of non-equilibrium phases, such as supersaturated solid solutions, metastable intermediate phases as well as quasicrystal and nanostructured materials [10,11]. Silica in nano form is used to improve the effectiveness, texture and preservation of various products [12,13]. Iron, however, has very potent magnetic and catalytic properties. Recently, much research interest has been shown to make the most of iron's potential, and work in this field seems to be blossoming. The binary Fe-Co is a soft magnetic alloy, whereas the addition of Ni in Fe enhances the electrical resistivity and permeability [14]. Hence, the ternary Fe-Co-Ni exhibits good soft magnetic properties, which makes this alloy suitable for several technological devices like magnetic recording media and magnetic fluids [15-17]. Very recently, the quinary system $Fe_{25}Co_{25}Ni_{25}(B,Si)_{25}$ [18] and the senary $Fe_{25}Co_{25}Ni_{25}(P,C,B)_{25}$ [19] high-entropy bulk metallic glasses (HE-BMGs) have been synthesized by the copper mold casting method, exhibiting good soft magnetic and mechanical properties. On the other hand, Wei et al. [20] successfully synthesized a senary $Fe_{26.7}Co_{28.5}Ni_{28.5}Si_{4.6}B_{8.7}P_3$ (HEA) by the melt spinning method, which formed an amorphous phase at high cooling rate and an FCC solid solution at low cooling rate.

In this paper, the FeCoNi and the FeCoNiSi alloy powder was prepared by mechanical alloying. To study the microstructural evolution and the effect of silicon especially on the structural parameters, a small amount of powder was collected after different milling times and examined by X-ray diffraction, using CuKα radiation (L=0.15418 nm). The synthesized material by mechanical milling is usually under far-from-equilibrium conditions, containing metastable crystalline, quasi-crystalline or amorphous phases, all which, either alone or in combination, make the material highly metastable. That is why the study of the transformation of these milling powders to the equilibrium state by thermal treatments was our second objective.

EXPERIMENTAL

The FeCoNi nanostructured alloy was synthesized starting from 50% Fe (99.7% purity), 25% Co (99.0% purity) and 25% Ni (99.7% purity) all by mass, and from 50% Fe (99.7% purity), 25% Co (99.0% purity), 15% Ni (99.7% purity) and 10% Si (99.9% purity) to synthesize the FeCoNiSi nanostructured alloy. The mixture powders were milled using a planetary-type ball mill Fritsch P7 in an

†To whom correspondence should be addressed.
E-mail: daly.rakia@gmx.fr

argon atmosphere. The milling was at different milling times, which stood at 100 h. To prevent excessive temperature rise inside the jars, milling was interrupted for 5 minutes after every 10 min. The ball-to-powder weight ratio was maintained at 1 : 2 and the milling speed was adjusted to 600 rpm. To study structural evolution, X-ray diffraction tests were performed with a Siemens D-500 using CuKα radiation. Concerning the phase identification, it was performed using PANalytical HighScore Plus© software (V4.5), which interfaces with the International Centre of Diffraction Data (ICDD) PDF4+ database. The crystallite size parameter was deduced from the X-ray diffractograms using the Rietveld method [21]. The calorimetric measurements were performed by Mettler-Toledo differential scanning calorimetry (DSC) 822 in a flowing argon atmosphere in the temperature range of 25-700 °C and at a heating rate of 10 °C/min.

RESULTS AND DISCUSSION

Fig. 1 and Fig. 2 show the X-Ray diffraction patterns of the FeCoNi and FeCoNiSi powder mixtures as a function of the milling time. The X-ray patterns of the unmilled powders display the Bragg diffraction peaks of the body-centered cubic (BCC)-Fe (Ref. ICDD Code: 03-065-4899), face centered cubic (FCC)-Ni (Ref. ICDD Code: 00-004-0850), hexagonal close-packed (HCP)-Co (Ref. ICDD Code: 01-089-7373) and cubic Si (Ref. ICDD Code: 01-080-0018). When process milling progresses, the peaks become more asymmetric and wider; in parallel, new peaks assigned to a structure of HCP-Co when it undergoes an allotropic conversion to FCC-Co (Ref. ICDD Code: 00-015-0806) appear, after 2 h of milling for the FeCoNiSi alloys and after 4 h of milling for the FeCoNi alloys, as it is demonstrated by the XRD Rietveld refinement.

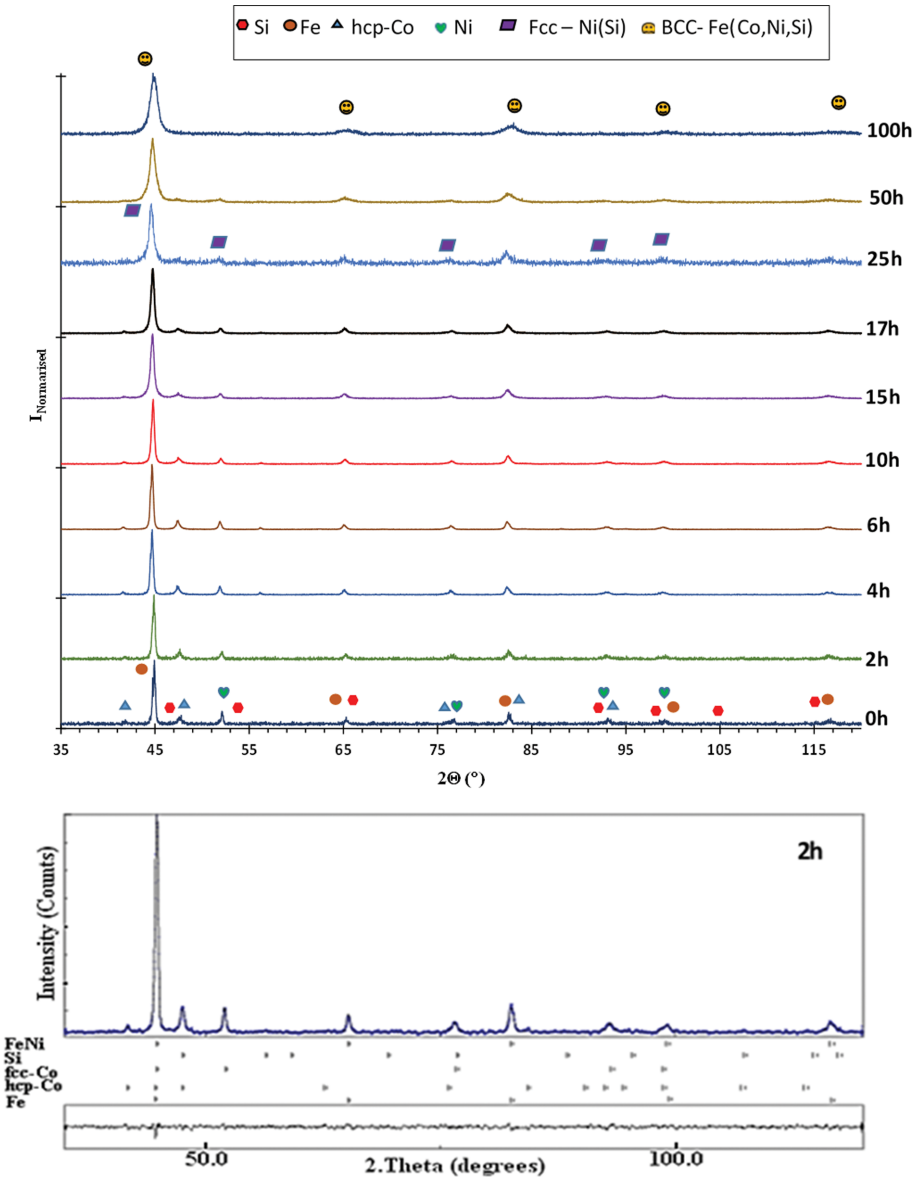

Fig. 1. X-ray diffraction pattern of the FeCoNiSi powder mixtures as a function of the milling time and the Rietveld refinement of XRD pattern for 2 h of milling.

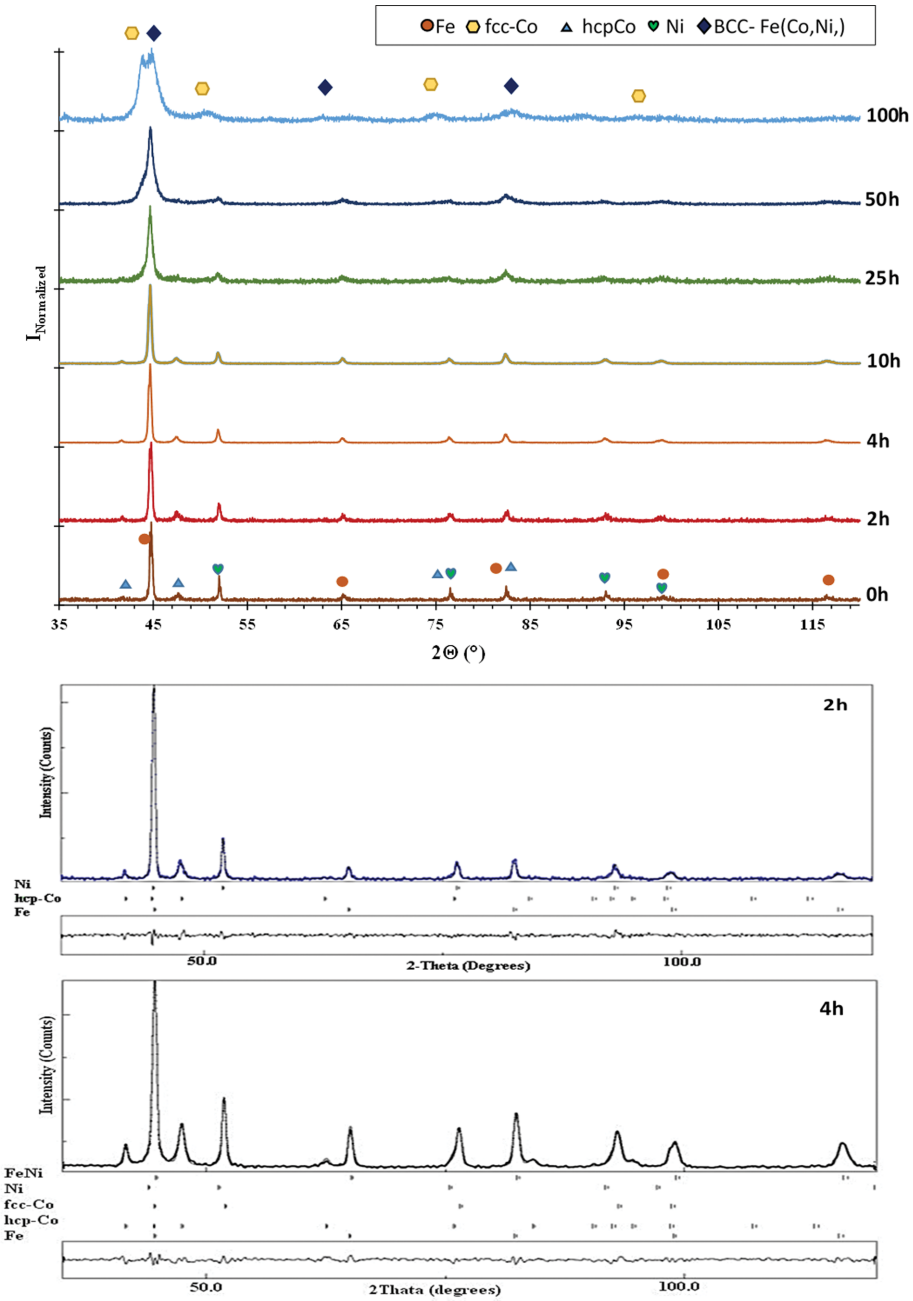

Fig. 2. X-ray diffraction patterns of the FeCoNi powder mixtures as a function of the milling time and the Rietveld refinement of XRD pattern for 2 h and 4 h of milling.

This time lag corresponding to this allotropic transformation between the two alloys depends on the grain size evolution during the milling process [22]. In fact, when the grain size is larger, the stable structure is HCP. Once a certain grain size has been reached, the stable structure becomes FCC. This is in accordance with the decrease of crystallite size with milling times as mentioned in Fig. 3. Indeed, for the FeCoNiSi, the sample greater reduction is observed, seemingly revealing that the Si rises the reduction rate of crystallites size by its hardener role, which causes microstructure fragility [23]. Hence, the crystallite size achieved after 25 h of milling reaches a value of 25 nm in comparison with FeCoNi, which has a value of 35 nm.

Dislocations are of paramount importance in the refinement of grains. In fact, the initial stages of deformation are characterized by the presence of dislocation cell blocks, which are separated by heavy dislocation walls, with dislocations arranged in a cellular way inside the blocks. As the strain increases, the cell blocks refine in size to become close to the cell size, the density of heavy dislocation walls increases, and the internal dislocation structure becomes more random with less space for cellular structures. Moreover, dislocation has an important role in the generation of a good mechanical and physical property of nanocrystalline material. Actually, it facil-

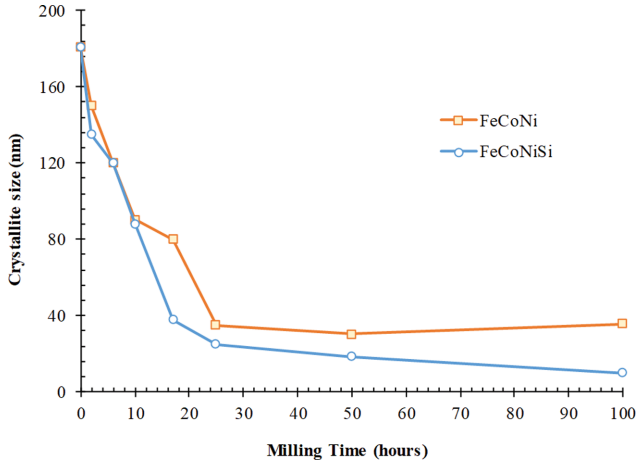

Fig. 3. Evolution of crystallite size as a function of milling time for the FeCoNi and FeCoNiSi alloys.

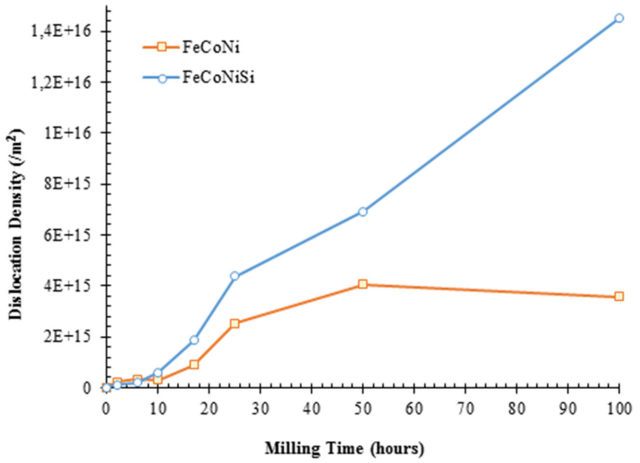

Fig. 4. Evolution of dislocation density as a function of milling time for the FeCoNi and FeCoNiSi alloys.

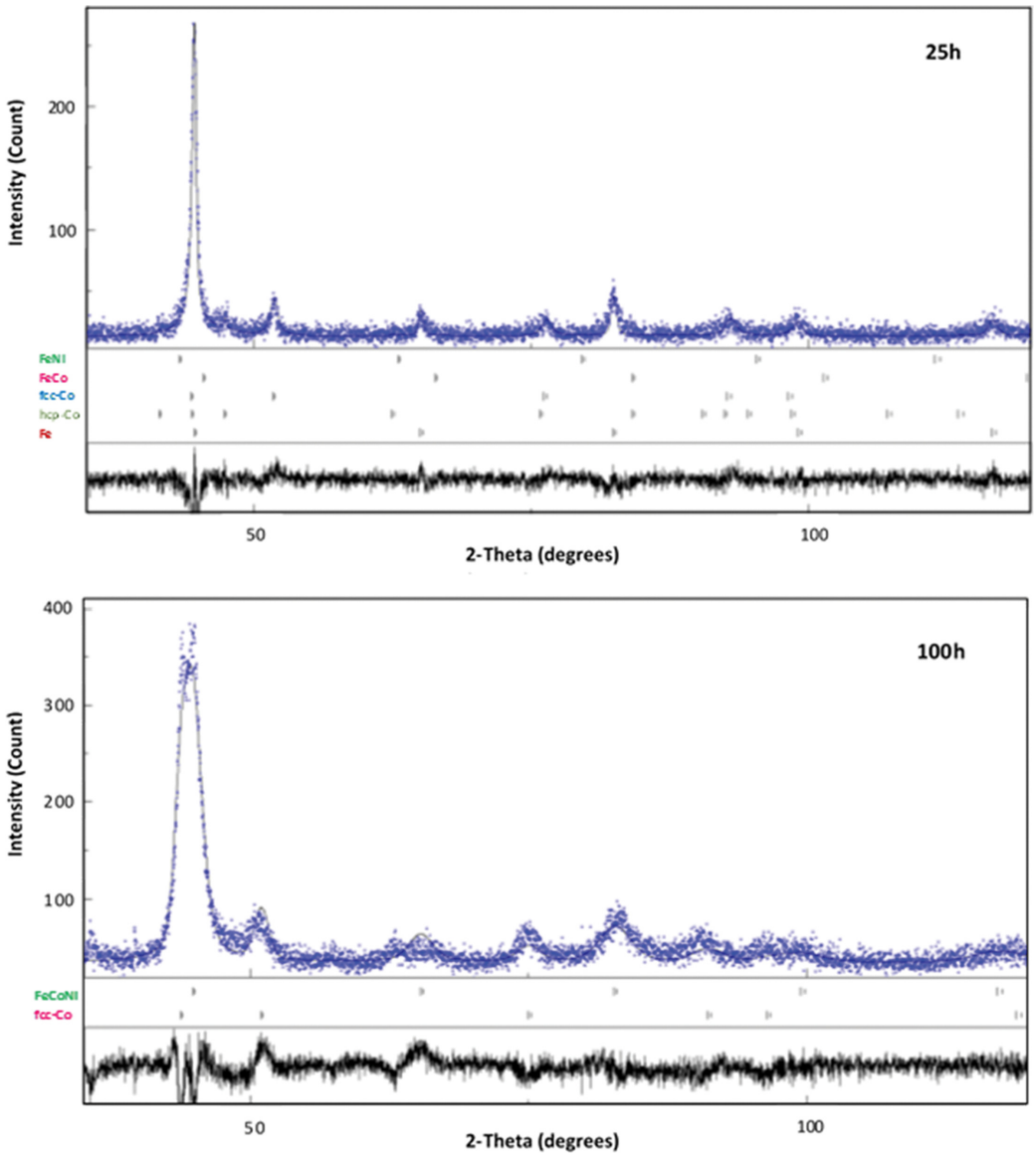

Fig. 5. The Rietveld refinement of XRD pattern of FeCoNi powders milled for 25 h and 100 h.

itates the formation of alloys and supersaturated solid solutions by accelerating the diffusivity of solute atoms. The density of dislocations is given by Eq. (1) [24,25]:

$$\sigma_d = 2\sqrt{3}\frac{\langle \varepsilon^2 \rangle^{1/2}}{Db} \quad (1)$$

where (D) is the crystallite size, (ε) corresponds to the microstrain, and b represents the Burgers vector of dislocations equal to ($a\sqrt{3}$)/2 for a BCC structure.

At can be seen in Fig. 4, the dislocation density reaches $1.13.10^{14}$ m^{-2} after 2 h of milling and increases up to $3.56.10^{15}$ m^{-2} after 100 h for FeCoNi alloy, while it is more important for FeCoNiSi alloy, attaining the value of $1.45.10^{16}$. The increase of the dislocation density is due to the hardening of the material by the diffusion of Co, Ni and Si in the iron matrix followed by the formation of solid solutions. Grain boundaries are used as barriers to dislocation movement, in the sense that when they turn hard or contract, the number of dislocations near the grain boundaries will increase. It is clear from the data that the dislocation density with the Si presence, is consistently higher than that of the FeCoNi alloy, which provides evidence that the introducing of silicon limits dislocation movement.

On the other hand, the shift of the most intense Fe peak to the high angle of Theta for the FeCoNi sample, notably after 25 h of milling can be explained by the diffusion of Co and Ni in Fe matrix and the formation of a supersaturated solid solution after 100 h of milling along with FCC-Co phase, as depicted in Fig. 5.

However, for the FeCoNiSi alloy, when the milling process progresses, the peaks become asymmetric and wide. Some of them will eventually disappear after 25 h of milling as Si and Ni peaks. In parallel, new solid solution phases are formed emanating from the diffusion of Ni, Co and Si in the Fe matrix; the complete dissolution of all the elements in Fe matrix leads to BCC-Fe (Co, Ni, Si) solid solution that was achieved at 100 h of milling as shown

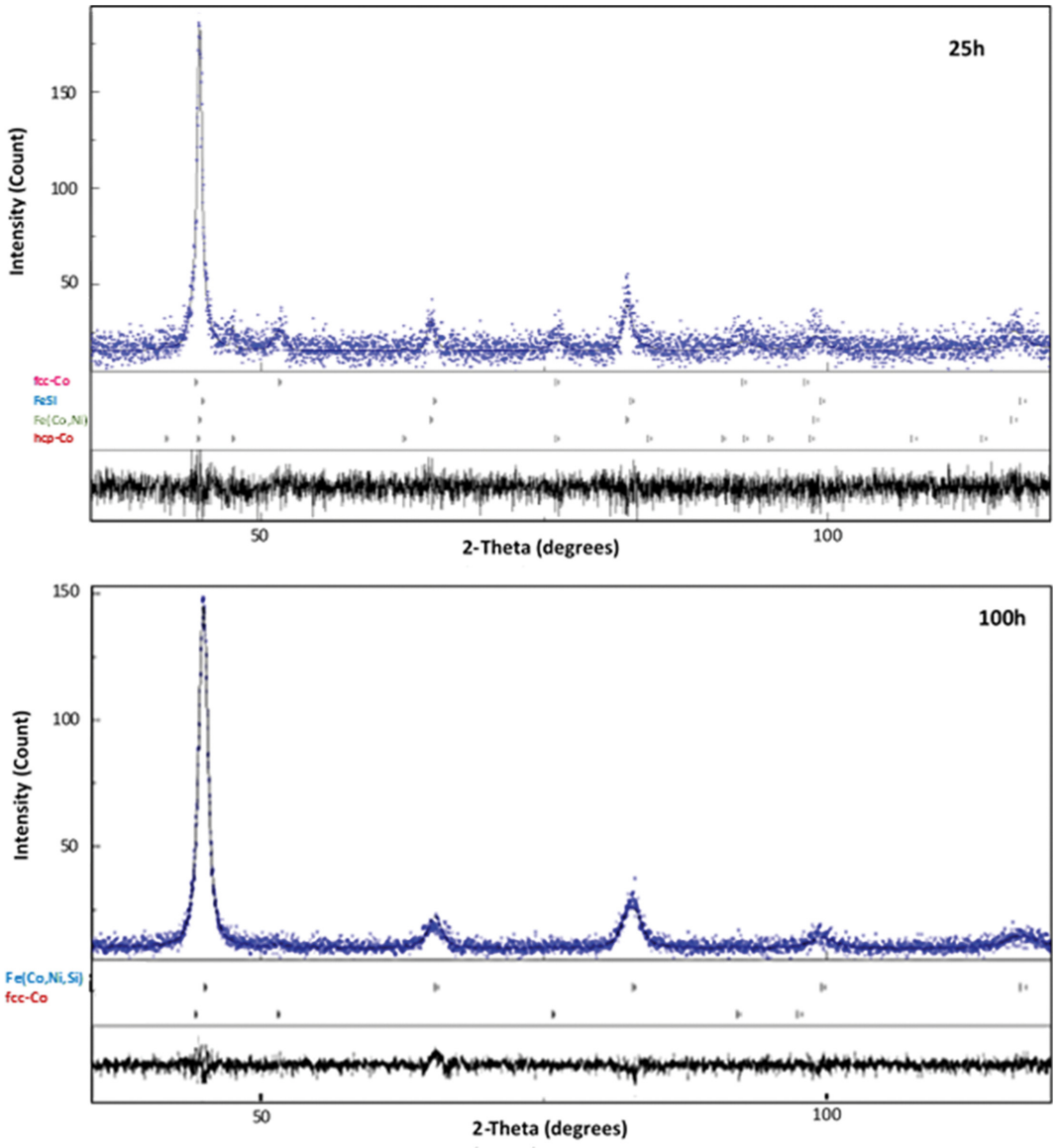

Fig. 6. The Rietveld refinement of XRD pattern of FeCoNiSi powders milled for 25 h and 100 h.

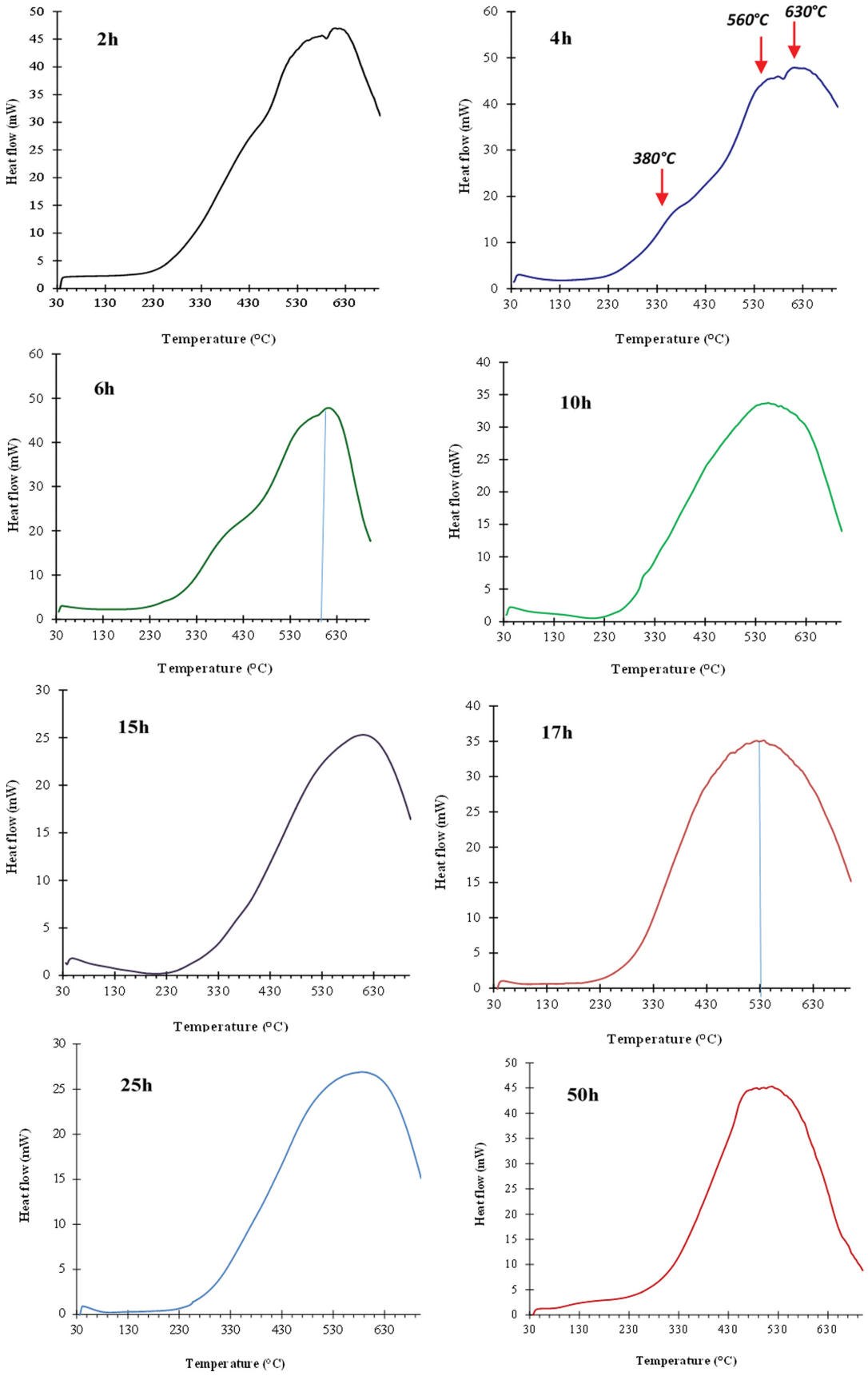

Fig. 7. DSC scans corresponding to the high-entropy alloy powder FeCoNi milled for 2 h, 4 h, 6 h, 10 h, 15 h, 17 h, 25 h and 50 h. Heating rate: 10 °C/min^{-1}.

by the results of the XRD Rietveld refinement in Fig. 6.

Fig. 7 shows the DSC curves of the FeCoNi alloyed powder milled at different times. The curves exhibit exothermic trends in the temperature range of 30-700 °C. The long exothermic line in the temperature range of 310 °C to 470 °C is associated with the release of internal stresses, such as structural deformation an lattice strain. Among others, an exothermic peak near 300 °C can be attributed to the small amount of oxidized cobalt [26] or further in the temperature range of 450-500 °C to the allotropic transformation of HCP-Co to FCC-Co [27]. The two exothermic peaks over 500 °C are related to the energy release during the phase transformation process, the formation of intermediate phases and grain growth. These peaks are seen to retreat to smaller temperature with the increased in milling time, indicating less stable phases; they also become weaker and more indistinguishable with the increase in milling up to 10 h.

To determine the origin of these exothermal peaks, while the alloy milling for 4 h was annealed up to 1 h at 310 °C, 590 °C and 680 °C, as revealed by Fig. 8, the one lasting for 50 h was annealed up to 1 h for 250 °C and 680 °C. After milling for 4 h and annealing at 310 °C, the formation of iron oxide Fe_3O_4 (Ref. ICDD Code: 00-002-1035) with a lower proportion was noticed. In fact, for the iron-oxygen system, the FeO (Wistite) phase reaches its stability at a temperature higher than 570 °C [28]. Below this temperature, it decomposes into iron and magnetite ($8FeO \rightarrow 2Fe+2Fe_3O_4$). The diffractogram of the same powder annealed at 590 °C shows the appearance of an FCC structure secondary phase $FeNi_3$ (Ref. ICDD Code: 01-088-1715). At 680 °C annealing leads to the decomposition of the compound into two phases: FeNi (Ref. ICDD Code: 00-018-0645) phase of cubic structure and FeCo (Ref. ICDD Code: 03-065-6829) phase next to the formation of FeO (Ref. ICDD Code: 01-088-1715) and Fe_2O_3 (Ref. ICDD Code: 00-013-0534) iron

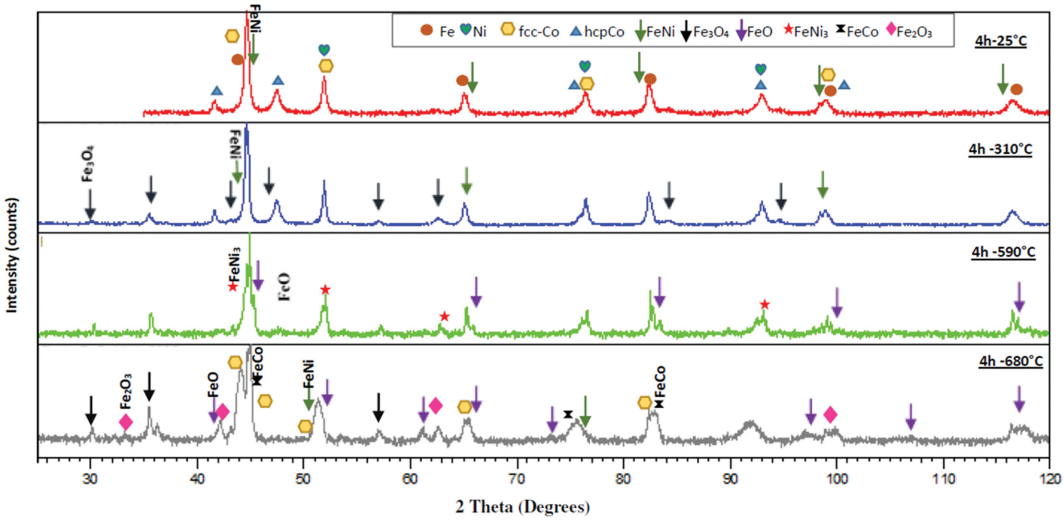

Fig. 8. X-ray diffractograms of as-milled (4 h) FeCoNi alloy and annealed powders at different temperature.

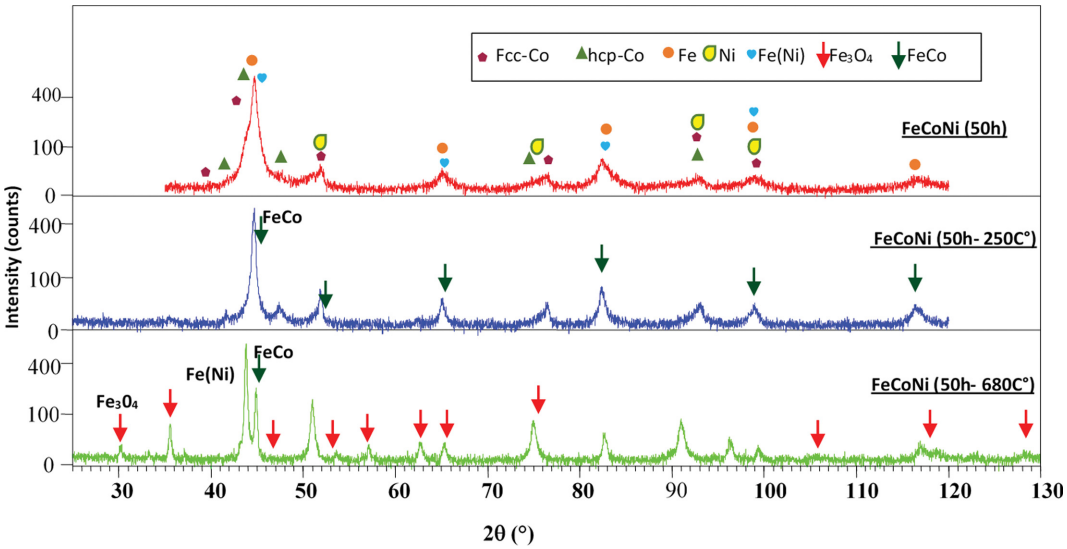

Fig. 9. X-ray diffractograms of as-milled (50 h) FeCoNi alloy, and annealed powders at different temperature.

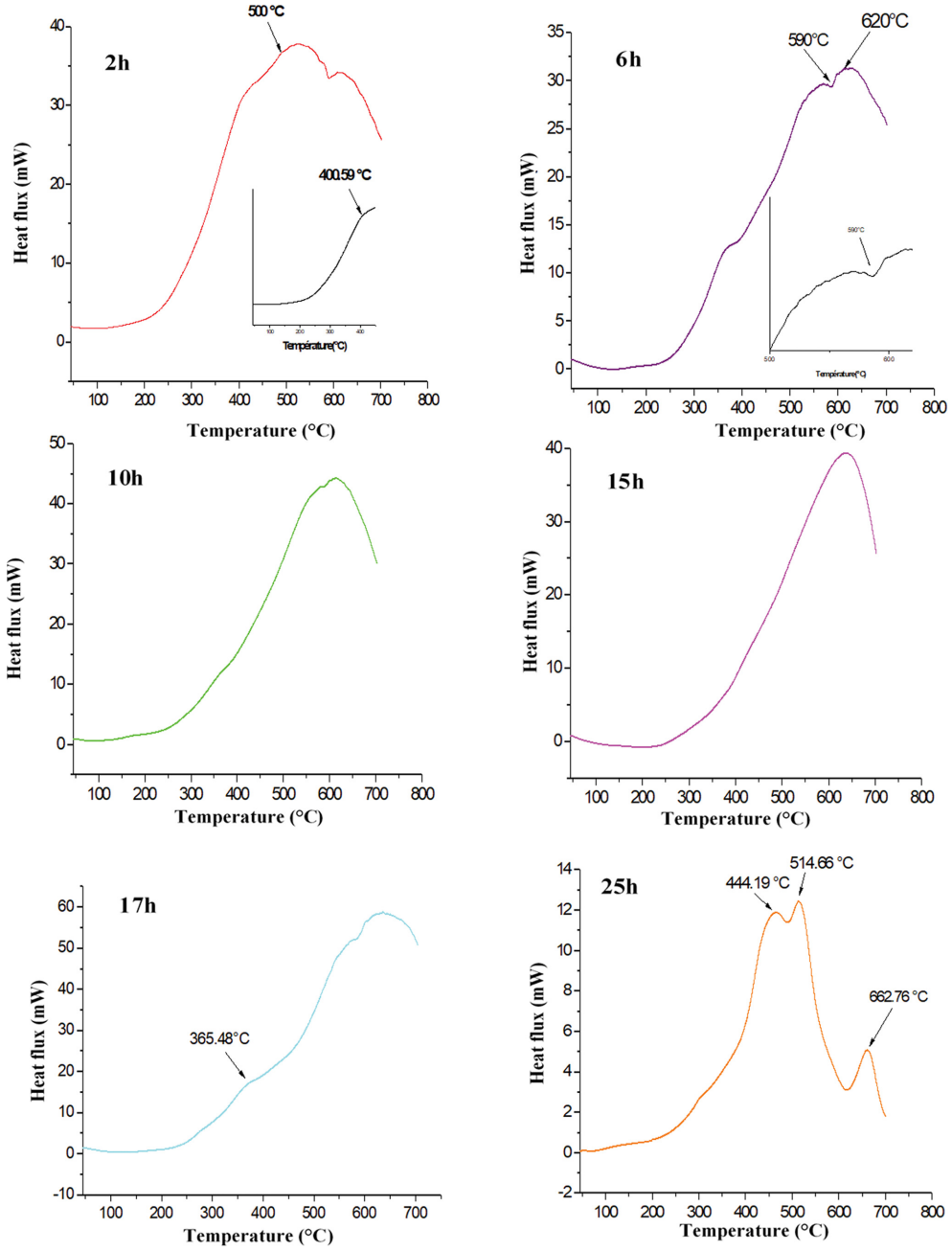

Fig. 10. DSC curves of the high-entropy alloy powder FeNiCoSi at different hours of milling Heating rate: 10 °C min^{-1}.

oxides.

For the powder milling up to 50 h, the diffractograms obtained after annealing at 250 °C reveal the formation of FeCo (Ref. ICDD Code: 03-065-6829) ascribed to the increase of internal energy by thermal heating, While annealing at 680 °C leads to the formation of the compound FeNi accompanied by the oxidation of the powder particles to form the iron oxide Fe_3O_4 as displayed in Fig. 9.

Fig. 10 shows the DSC scans of FeCoNiSi alloy milled for 2, 6, 10, 15, 17 and 25 h. Several exothermic processes were detected on heating. There is a broad hump beginning at about 290 K associated with the relief of internal stresses. The powder milling for 25 h reveals three exothermal peaks located in the DSC curve in the temperature range of 444 °C, 514 °C and 662 °C. To determine the origin of these exothermal peaks, annealing experiments on 25 h milled sample were carried out at different temperatures of 290 °C, 400 °C, 480 °C, 610 °C and 700 °C. The phase composition of annealed samples was analyzed by X-ray diffraction and the results are exhibited in Fig. 11. It can be clearly noted that an annealing at 290 °C and 400 °C leads to a regeneration of several phases, such as NiSi (Ref. ICDD Code: 00-003-1085), FeSi (Ref. ICDD Code: 01-089-2677 and SiCo (Ref. ICDD Code: 01-072-1328).

However, the 480 °C-annealed XRD pattern suggests the appearance of FeCoNi (Ref. ICDD Code: 04-016-6385 and FeSiCo (Ref. ICDD Code: 03-065-8930) phases, the formation of iron oxide and

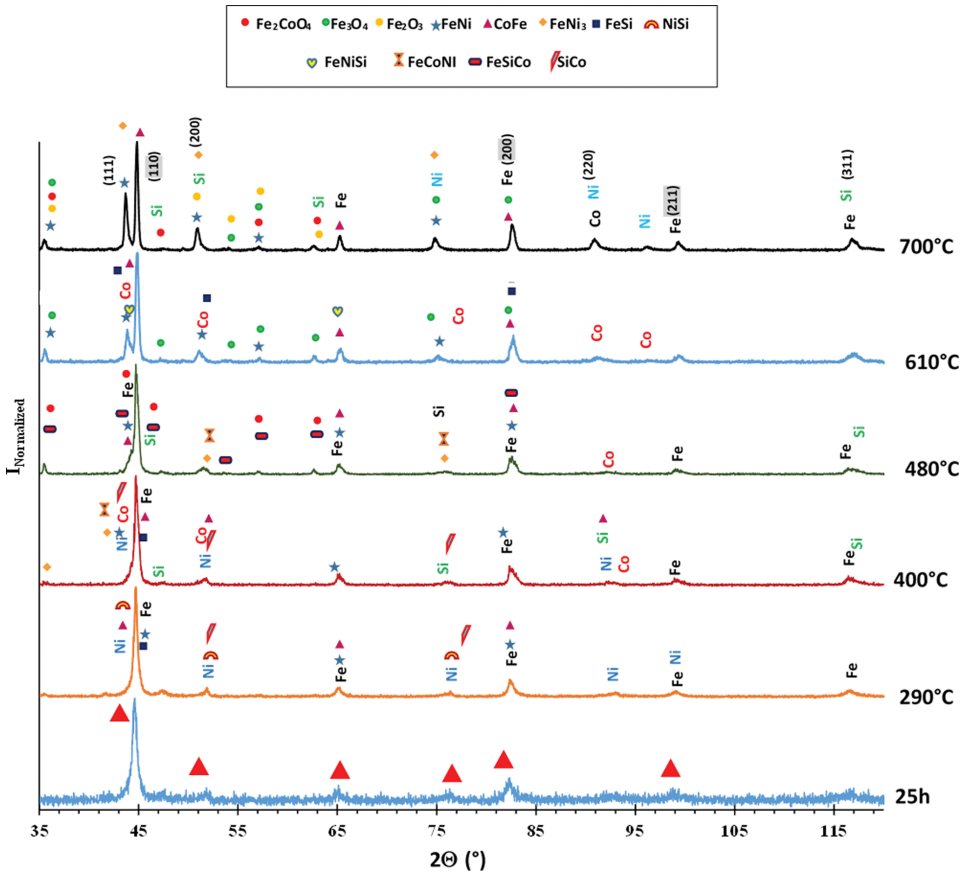

Fig. 11. X-ray diffractograms of as-milled (25 h) FeCoNiSi alloy, and annealed powders at different temperature.

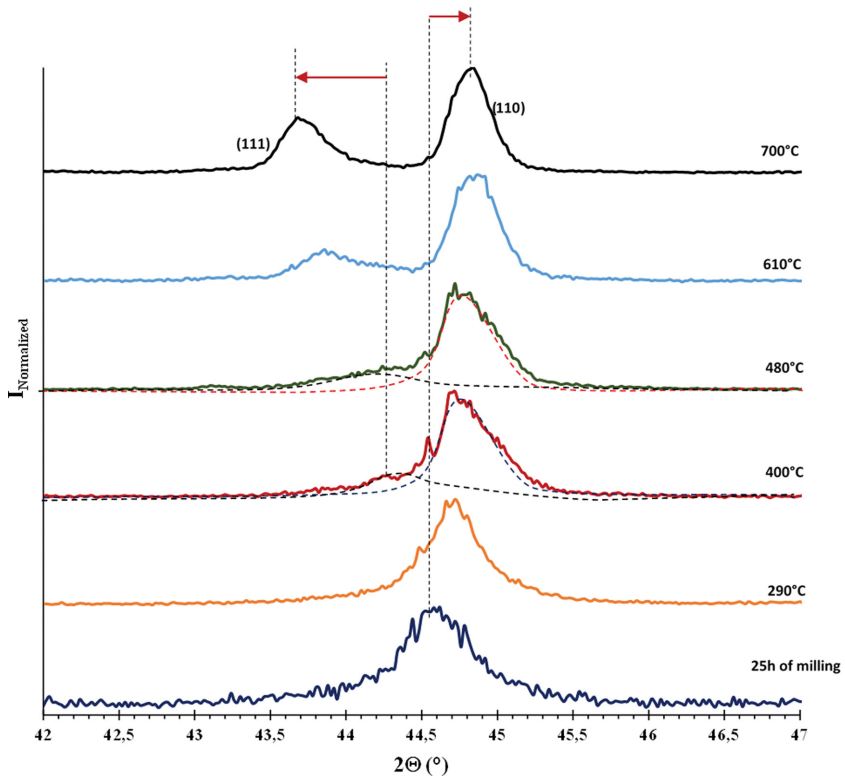

Fig. 12. X-ray diffractograms of the (111) and (110) peaks of the annealed FeCoNiSi powders at different temperature.

the generation of a cubic crystal structure Fe_2CoO_4 (Ref. ICDD Code: 00-001-1121), along with the broadening of the (110) peak which becomes sharper and shifts towards a higher angle. Note that after annealing at 610 °C, there is the formation of Fe_3O_4 generated by the decomposition of FeO. The FeCo and FeNi phases with BCC phase and FCC structure are separated from the matrix when the annealing reaches 700 °C. The intensity of (111), (200) and (220) for FCC was found to increase, which is attributed to the augmentation of crystallinity. Nevertheless, BCC corresponding to (110), (200) and (211) crystal face starts to precipitate.

Fig. 12 shows an enlarged picture of the main FCC and BCC peak positions, and the shift of the (111) peak to the low values of theta when the intensity of the diffraction peaks increases, due to the increase in crystallinity and crystallite size and the decrease in the internal stress of the alloy powders.

CONCLUSION

Soft nanostructured FeCoNi and FeCoNiSi alloys were developed after 100 h of mechanical milling. We observed the formation of nanoscale iron-based supersaturated solids: Fe(Co,Ni) and Fe(Co,Ni,Si). This formation of solid solutions was accompanied by the allotropic transformation HCP-Co→FCC-Co. The structure of the defects is considered to be responsible for the refinement of microstructure at the nanometer size. Furthermore, silicon has an important role in the increase of structural hardening and subsequently the more pronounced refinement of crystallites. The analysis of the thermal stability of the mixture powders as a function of milling time demonstrated the succession of the exothermic transformations that accompany the restoration of the deformed microstructure, the recrystallization of new phases and coarsening of the alloy grains.

REFERENCES

1. N. K. Prasad and V. Kumar, *J. Mater. Sci. Mater. Elect.*, **26**, 10109 (2015).
2. H. Raanaei, H. Eskandari and H. V. Mohammad, *J. Magn. Magn. Mater.*, **398**, 190 (2016).
3. A. Zeleňáková, D. Olekšáková, J. Degmová, J. Kováč, P. Kollár, M. Kusý and P. Sovák, *J. Magn. Magn. Mater.*, **316**, e519 (2007).
4. C. Suryanarayana, *Prog. Mater. Sci.*, **46**, 1 (2001).
5. E. Jartych, *J. Magn. Magn. Mater.*, **323**, 209 (2011).
6. T. Pikula, D. Oleszak, M. Pękała and E. Jartych, *J. Magn. Magn. Mater.*, **320**, 413 (2008).
7. G. M. Mocolvin and M. J. Shaw, *Mater. Sci. Forum*, **88**, 235 (1992).
8. G. B. Schaffer and P. G. McCormick, *Appl. Phys. Lett.*, **1**, 45 (1988).
9. B. Avar and S. Ozcan, *J. Alloys Compd.*, **650**, 53 (2015).
10. C. Suryanarayana, *Int. Mater. Rev.*, **40**, 41 (1995).
11. C. Suryanarayana, *Prog. Mater. Sci.*, **46**, 1 (2001).
12. M. R. Kasaai, *J. Nanotechnol.*, **4**, 1 (2015).
13. C. A. Poland, P. B. Larsen, S. A. K. Read, J. Varet, S. M. Hankin and H. R. Lam, D.E.P.A: Copenhagen, Denmark, 23 (2016).
14. A. C. Santos, F. Morais, A. Simões, I. Pereira, J. A. D. Sequeira, M. Pereira-Silva, F. Veiga and A. Ribeiro, *Expert Opin. Drug Deliv.*, **16**, 313 (2019).
15. D. Jiles, *Introduction to magnetism and magnetic materials*, Chapman and Hall/CRC Press: New York, NY, USA (1998).
16. H. Raanaei, H. Eskandari and V. Mohammad-Hosseini, *J. Magn. Magn. Mater.*, **398**, 190 (2016).
17. X. Li and S. Takahashi, *J. Magn. Magn. Mater.*, **214**, 195 (2000).
18. Q. I. Tianlong, L. I. Yanhui, A. Takeuchi, X. Guoqiang, H. Miao and W. Zhang, *Intermetallics*, **66**, 8 (2015).
19. Y. Li, W. Zhang and T. Qi, *J. Alloys Compd.*, **693**, 25 (2017).
20. R. Wei, H. Sun, C. Chen, Z. Han and F. Li, *J. Magn. Magn. Mater.*, **435**, 184 (2017).
21. V. Petrisek and D. M. Jana, The Crystallographic Computing System (Institute of Physics), Prague (2000).
22. E. A. Owen and D. Madoc Jones, University College of North Wales, Bangor MS (1954).
23. P. Novák, M. Zelinková, J. Šerák, A. Michalcová, M. Novák and D. Vojtěch, *Intermetallics*, **19**, 1306 (2011).
24. G. K. Williamson and W. H. Hall, *Acta Metall.*, **1**, 22 (1953).
25. Y. Zhao, H. Sheng and K. Lu, *Acta Mater.*, **49**, 365 (2001).
26. L. D. Rafailović and D. M. Minić, *Chem. Ind.*, **63**, 557 (2009).
27. B. N. Mondal, A. Basumallick, D. N. Nath and P. P. Chattopadhyay, *Mater. Chem. Phys.*, **116**, 358 (2009).
28. D. Bruce and P. Hancock, *Br. Corros. J.*, **4**, 221 (1969).